https://doi.org/10.2352/ISSN.2470-1173.2019.11.IPAS-258

Phase masks optimization for broadband diffractive imaging

Mykola Ponomarenko, Vladimir Katkovnik, Karen Egiazarian
Tampere University, FIN 33101, Tampere, Finland

Abstract

The task of optimization of phase masks for broadband diffractive imaging to minimize chromatic aberrations and to provide given value of Depth of Focus (DoF) is considered. Different schemes of multilevel phase mask (MPM) forming by combining pixels of two Fresnel lenses are analyzed. The Fresnel lenses are calculated for the same focal distance but for very different wavelengths. A possibility of adding to the optimized mask a cubic component is taking into account as well as usage of discrete phase masks with optimized number of levels. It is shown that the proposed approach in the combination with inverse imaging allows to significantly increase image quality for a focus distance in comparison to refractive lens-based optical systems. Moreover, it is shown that by changing of aforementioned parameters it is possible to increase or decrease DoF value depending from a given goal of optimization. It is demonstrated by numerical analysis that the proposed approach significantly increases robustness of designed MPM to Gaussian additive noise in MPM introduced due to fabrication errors.

Keywords: Lensless imaging, multilevel phase mask design, inverse imaging, diffractive optical elements

Introduction

Optical systems with diffractive imaging [1] are an alternative of refractive optics thanks to their compactness, low cost and smaller light losses (in comparison to multilens optical systems).

The main area of usage of diffractive optics is monochromatic light systems, but recent publications show many ways of their usage in broadband (full spectrum) imaging [2].

The considered optical system is shown on the Fig. 1. Here d_1 is a distance between a scene and a phase mask, d_2 is a distance between the phase mask and a sensor. An image on the sensor is more blurred than for lens-based refractive optical systems, but there is a possibility to obtain the image after an inverse imaging with better quality than the same one for lens-based optics.

It is shown that for broadband imaging a significant decreasing of chromatic aberrations can be reached using a wavefront coding with addition of a cubic phase mask [3].

There are two main problems of phase masks optimization.

First, selection of a quality criterion for the optimization is a difficult task. In some papers [4] phase mask are optimized to provide similar point spread functions (PSFs) of designed optical system for all wavelengths of visible range. Potentially it may decrease chromatic aberrations and increase effectiveness of inverse imaging. However it is not clear, which criteria of similarity of PSFs should be used? Moreover, one may obtain similar PSFs by the price of significant increasing of blur level of images on the sensor. This, in turn, will result in decreasing of quality of inverse imaging and increasing of its sensitivity to other distortions (noise and quantization). In other papers [5] PSNR or reconstructed image (image after inverse image) is used as optimization criterion. However, in this case the task is complicated by significantly larger amount of needed numerical analysis (for obtaining of a reliable statistic one should calculate the quality criterion for a number of test images). Moreover, this quality criterion is vector, because PSNR for reconstructed images should be calculated for different values of defocusing parameter). Therefore, one should select a rule for estimation of optimality of such vector criterion and the rule will be heuristic.

Second, the phase mask is a two dimensional array, which may contain hundreds of thousands or even millions of pixels. A pixel wise optimization of such mask is computationally impossible. Because of this on a practice such optimization usually is simplified to optimization of levels of concentric rings or size of sectors of the mask. However quality of images obtained using masks optimized in this way are low for most of practical applications.

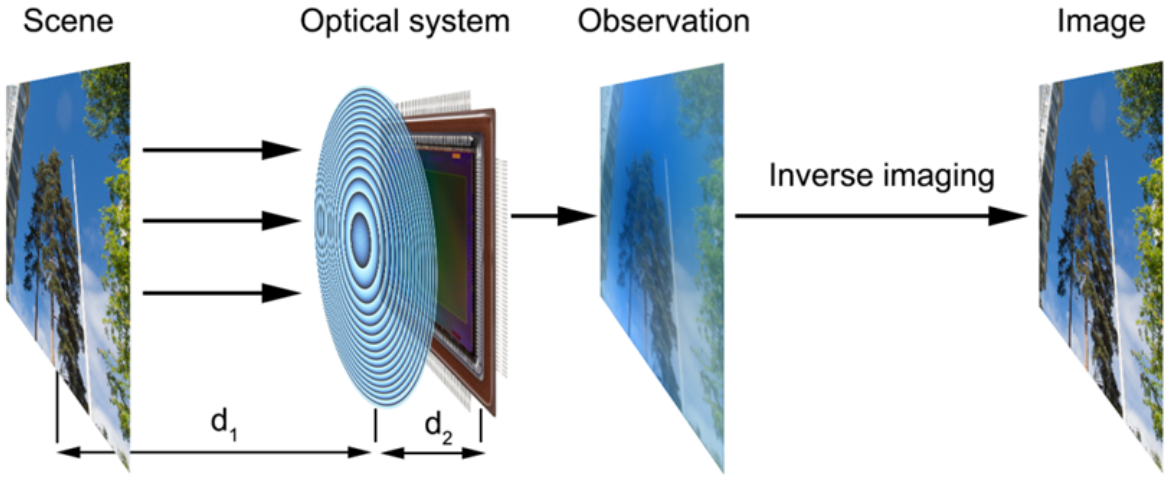

Fig. 1. A lensless camera with phase modulation diffractive MPM and inverse computational image restoration

In our paper [5] we propose to limit the mask optimization by optimization of several parameters: base wavelength, level of cubic phase component, number of levels of discrete phase mask, mask pixel size. This approach allows to extend DoF value of a designed optical system and to decrease chromatic aberrations for a focus distance. However, this approach does not allow to solve task of decreasing DoF value. Moreover, results of optimization depend from used set of test images, because optimization curves are indented and have many extremums.

In the paper we propose a new approach which allows to combine two phase masks on the base of Fresnel lenses with the same focal distance but calculated for two different wavelengths. The approach also allows to increase or to decrease DoF value of a designed optical system by varying of these wavelengths, proportion of pixels of Fresnel lenses in the formed phase mask, and level of a cubic phase component. The approach provides a low level of blur and chromatic aberrations on reconstructed images. At the same time, number of optimization parameters in comparison to [5] is increased only on one or two parameters which is acceptable from computational point of view.

Two different schemes of combination of Fresnel lenses are considered: regular and random. It will be shown that the random one is more robust to presence a noise in MPM.

Diffractive image formation

The optics of the considered setup (Fig. 1) consists of a very thin diffractive mask (MPM in our case) which is parallel to the sensor. A distance d_2 between the sensor and optics is much smaller than the object-to-optics distance d_1 (Fig. 1). Due to the MPM, the object is imaged on the sensor as a blurred pattern. A computational inverse imaging is used for reconstruction of the sharp object image from the recorded blurred one.

The corresponding singlet optical scheme is shown on the Fig.2: object plane with coordinates (ξ, η), optical element (MPM) plane (x, y) and sensor array plane (u, v). The f_0 is a focal distance of the lens used as a design parameter of the lensless system.

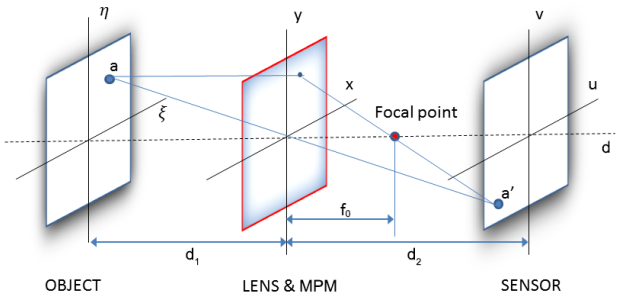

Fig. 2. Singlet optical setup with MPM in the pupil plane

Image formation using MPM can be accurately modeled by the scalar diffraction theory with the Fresnel approximation for wavefront propagation [6], [7].

The generalized pupil function P_λ of the considered optical system can be represented as:

$$P_\lambda(x,y) = P_A(x,y)\exp\left[\frac{j\pi(d_1+d_2)(x^2+y^2)}{\lambda d_1 d_2} + jMPM_{\lambda_0,\lambda}(x,y)\right], \quad (1)$$

where P_A is aperture, λ is wavelength, λ_0 is design wavelength, $MPM_{\lambda,\lambda 0}$ is phase delay enabled by MPM for the wavelength λ provided that the design parameter λ_0 is fixed.

Multilevel phase masks

According to the procedure proposed in [5], the design of MPM starts with introducing of some absolute phase taken of the form:

$$\varphi(x,y) = -\frac{\pi}{\lambda_0 f_0}\left(x^2+y^2\right) + \varphi_{GCPM}(x,y), \quad (2)$$
$$\varphi_{GCPM}(x,y) = \alpha\left(x^3+y^3\right) + \beta\left(x^2 y + y^2 x\right),$$

where φ_{GCPM} is a cubic component providing wavefront coding [8], [9].

In our design we will optimize only the α parameter setting β to zero.

An example of designed MPM with a cubic component is shown on the Fig. 3.

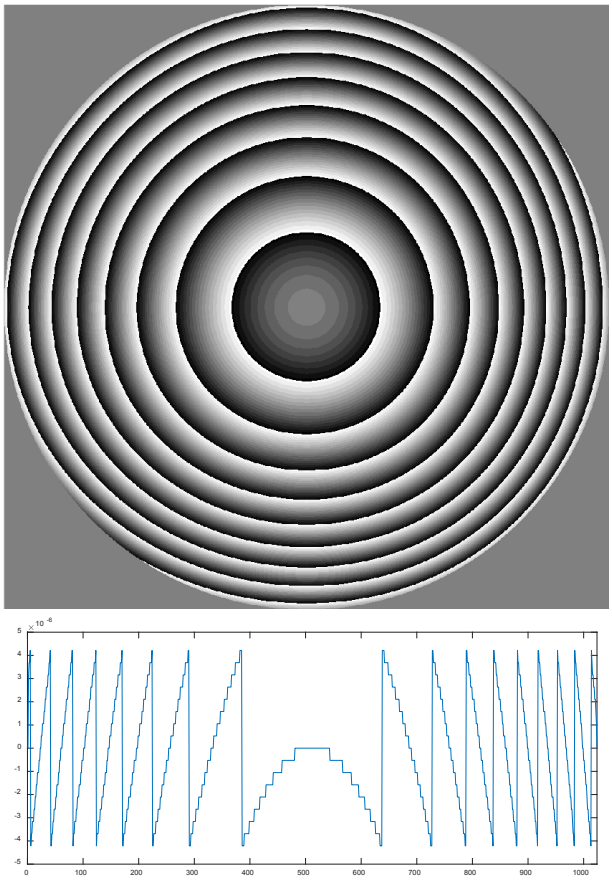

Fig 3. An example of MPM with a cubic component and its cross-section

it is clearly seen that such MPMs are unsymmetrical.

Inverse imaging

Flow chart of inverse imaging used in the paper is shown on the Fig. 4.

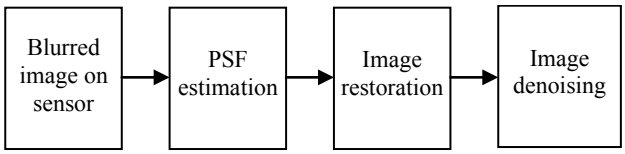

Fig. 4. Flow chart of used inverse imaging

The PSF of the coherent monochromatic optical system is defined as

$$\mathrm{PSF}_{\lambda}^{\mathrm{coh}}(u,v) = \mathrm{F}\,\mathrm{P}_{\lambda}\left(\frac{u}{d_2\lambda},\frac{v}{d_2\lambda}\right), \quad (3)$$

where $\mathrm{F}\,\mathrm{P}_{\lambda}$ stands for the Fourier transform of Pλ [6].

Following to [5] the broadband PSFs is the wavelength dependent PSFs averaged with the weights defined by $T_c(\lambda)$:

$$\mathrm{PSF}_C(u,v) = \frac{\int_{\Lambda} T_C(\lambda)\left|\mathrm{PSF}_{\lambda}^{\mathrm{coh}}(u,v)\right|^2 d\lambda}{\int\int_{-\infty}^{\infty}\int_{\Lambda} T_C(\lambda)\left|\mathrm{PSF}_{\lambda}^{\mathrm{coh}}(u,v)\right|^2 dudvd\lambda}. \quad (4)$$

The input-output image formation equations can be represented as convolutions:

$$I_{S,C}(u,v) \approx \int_{-\infty}^{\infty}\int_{-\infty}^{\infty} I_{O,C}(x,y)\mathrm{PSF}_C(u-x,v-y)dxdy, \quad (5)$$

where $I_{O,C}$ is the "ideal" narrow-band object image for c-channel in the RGB color space.

The equation (5) is used for reconstruction of Io;c from the observed $I_{S,C}$. A moving from $\mathrm{PSF}_{\lambda}(x, y)$ to $\mathrm{PSF}_c(x, y)$ makes the inverse imaging manageable because both the "ideal" object and observations are defined for the RGB space.

For calculation of the Fourier transforms (3) we use the technique proposed in [10]. It results in Matrix Discrete Fourier Transform (MDFT). For the grid (U, V) the MDFT calculation is carried out by the matrix multiplication:

$$\mathrm{PSF}_{\lambda}^{\mathrm{coh}}(u,v) = A_y P_g(X,Y) A_x. \quad (5)$$

An example of PSF_C calculated according to (4) is shown on the Fig. 5.

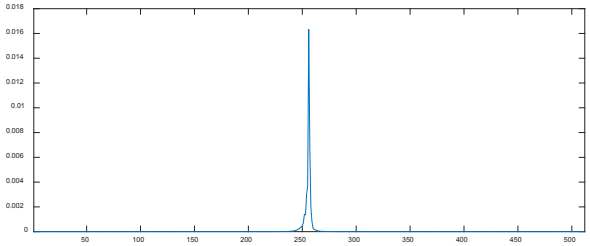

Fig. 5. An example of cross-section of calculated PSF_C

For deblurring, we use BM3DDEB algorithm [11], which is applied to each color channel separately.

Proposed design of multilevel phase masks

We considered different schemes of combining of two Fresnel lenses into an one phase mask and selected those that do not introduce in image on the sensor of geometric or local distortions. Only schemes, which provide more or less uniform blurring of image on the sensor, are included in further numerical analysis and optimization.

Fig 6. shows examples of two such combined phase masks: the diagonal combination of two Fresnel lens halves and the random combination of pixels two Fresnel lenses (in the proportion 1:1).

Both of the considered combined MPMs shows very similar performance. However, the random combination is more stable to noise presence (due to fabrication errors) and will be used in numerical analysis in the paper.

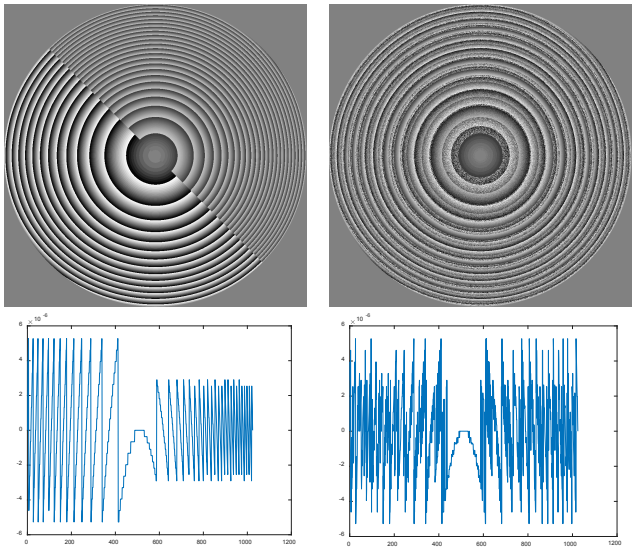

a b

Fig. 6. Considered combinations of two MPMs (One of them is calculated for λ_0=400 nm, second for λ_0=700 nm): a) diagonal combination (MPM and cross-section); b) random combination

In the paper we use monochrome sensor (without usage of color filters) with all T(λ) equal to unity, which is most difficult case for single lens imaging due to most wide range of wavelengths causing huge chromatic aberrations.

Fixed parameters of optical setup used in the paper are given in the Table 1.

Table 1. Parameters of optical setup

D, mm	f_0, mm	λ, nm	pitch, μm	sensor	d_1, m	d_2, mm
1.2	2.4	446...700	2.5	512x512	1	2.4

Optimization parameters are α, λ0 (separately for two component of combined MPM), thickness, number of MPM levels, width of steps in MPM.

Both MPM (with own α and λ0 values) are calculated according to (2) and methodology described in [5]. Than they are combined as on the Fig. 6, b.

For optimization ground truth multichannel images $I_{O,\lambda}$ are used. Ground truth images are calculated as

$$I_{O,C}(u,v) \approx \int_{\Lambda} I_{O,\lambda}(x,y)T_C(\lambda)d\lambda, \quad (6)$$

where all $T_C(\lambda)$ in the paper are equal to unity (we use a monochrome sensor). So (6) can be simplified to

$$I_{O,C}(u,v) \approx \int_{\Lambda} I_{O,\lambda}(x,y)d\lambda. \quad (7)$$

Having $I_{O,C}$ and observed $I_{S,C}$ (calculated in accordance to [5]) it is possible to calculate $\hat{I}_{O,C}(u,v)$ and PSNR as

$$\mathrm{RMSE} = \sqrt{\mathrm{mean}_{x,y,c}\left(\left[\hat{I}_{O,C}(u,v) - I_{O,C}(u,v)\right]^2\right)},$$
$$\mathrm{PSNR} = 20\log\frac{\max_{u,v,c} I_{O,C}(x,y)}{\mathrm{RMSE}}. \quad (8)$$

We consider PSNR as a function of the defocus parameter $\Delta d_2/d_2$, where Δd_2 is a deviation of the sensor plane from its precise position d_2. In our optimization, DoF is defined through the maximum length of the interval of $\Delta d_2/d_2$ values, provided that the corresponding PSNRs take the large enough values. A larger value of this interval means a larger DoF.

Numerical analysis

For numerical experiments, the high-quality remote sensing images from AVIRIS (Airborne Visible Infrared Imaging Spectrometer), NASA are used. Overall, the AVIRIS data-set consists of 224 channel images with $\Delta\lambda$ = 9.375 nm step between the channels. As ground truth data, four AVIRIS multichannel images (Moffett Field, Cuprite, Lunar Lake and Low Altitude) are selected (Fig. 7). From each image, we cut off 512x512 fragments containing multicolored sharp details and took 28 channels covering the wavelength range Λ = [446.875 700] nm with the wavelength step $\Delta\lambda$ = 9.375 nm.

PSNR is calculated in accordance to (8) for RMSE averaged for all four test images.

We consider three different setups. The first is randomly combined MPM. Optimized parameters are given in the Table 2. 1.

Table 2. Optimized parameters of randomly combined MPM

	λ_0, nm	α	Number of MPM levels	Pitch, μm	Width of steps
MPM #1	400	5	16	12	
MPM #2	700			5.5	

The second is the same MPM but in noisy environment. The MPM is distorted by Gaussian additive noise with σ = 100 nm (the noise simulates MPM fabrication errors).

An the third is single lens based optical system.

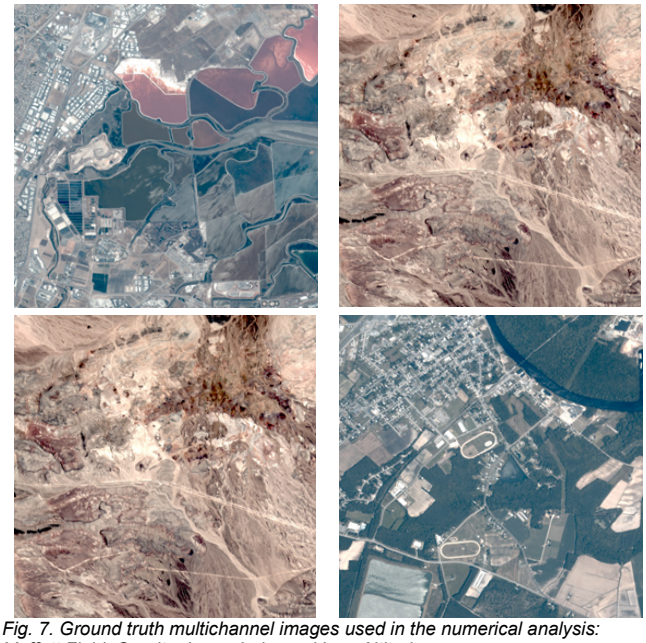

Fig. 7. Ground truth multichannel images used in the numerical analysis: Moffett Field, Cuprite, Lunar Lake and Low Altitude

Curves of dependence of PSNR from the defocus parameter $\Delta d_2/d_2$ for all compared setups are shown on the Fig. 9. It is well seen that despite of such a big noise "MPM+noise" setup provide PSNR values very close to the MPM optical system without noise.

In focus ($\Delta d_2/d_2$=0) the proposed MPM has PSNR bigger than for single lens system more than on 8 dB, providing also much more wider DoF.

Examples of images after inverse imaging for the proposed combined MPM and for single lens optical system are shown on the Fig. 10. It is clearly seen that even for a such a big defocusing the proposed MPM allows to made sharp images with a good visual quality.

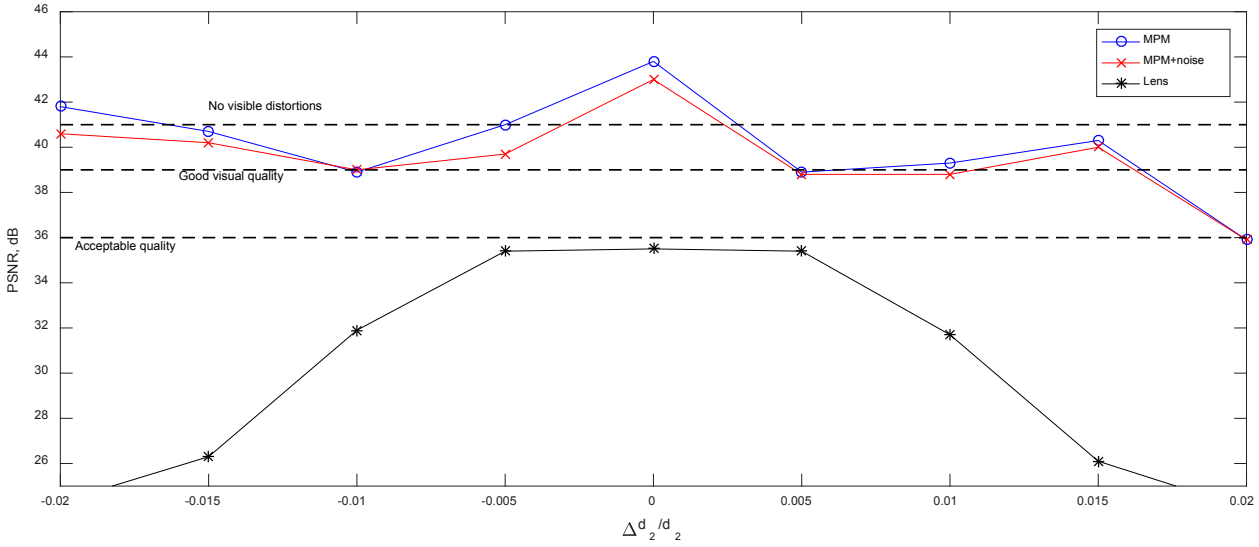

Fig. 9. PSNR for compared optical setups and noise environments for different defocus

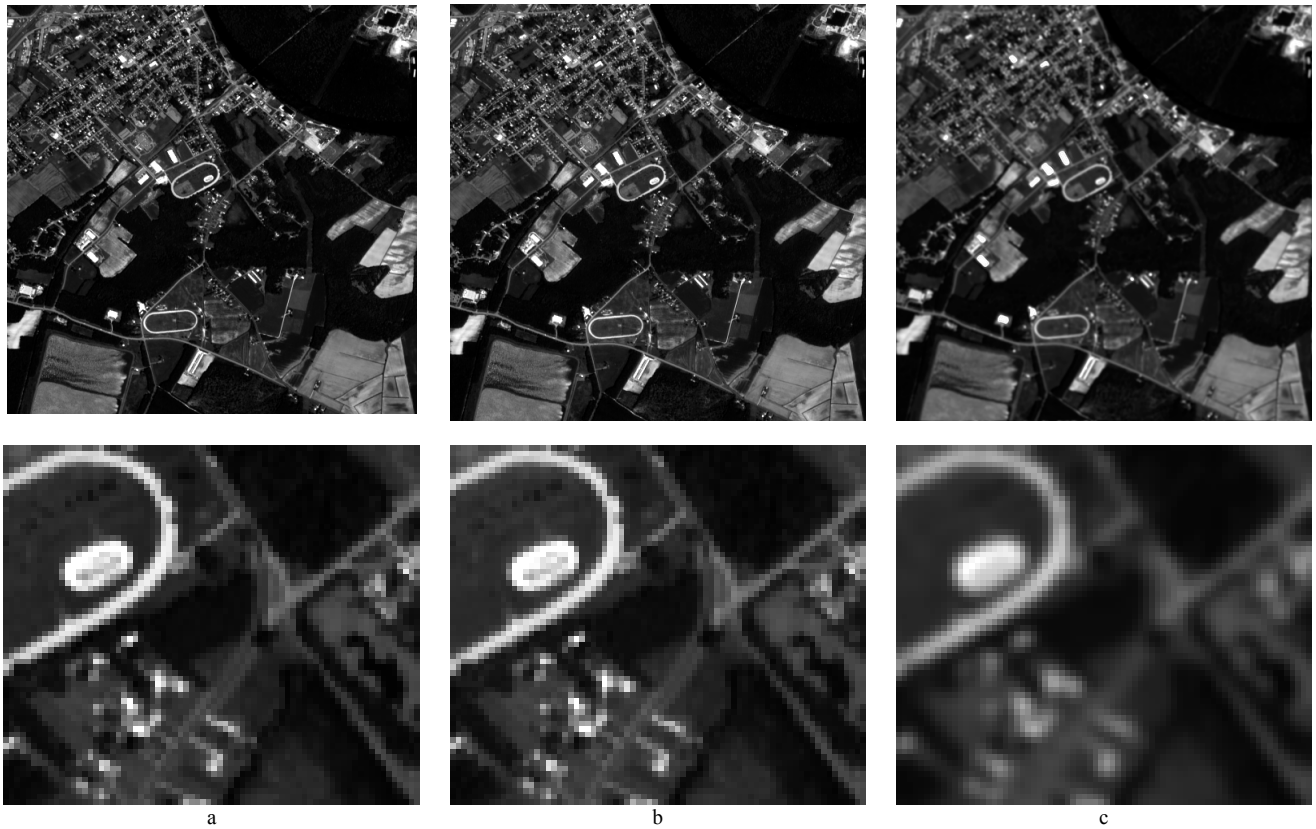

a b c

Fig.10. Visual comparisons: a) True image Low Altitude and its enlarged fragment; b) MPM, $\Delta d_2/d_2$=0.015, PSNR = 40.3 dB and its enlarged fragment; c) Lens , $\Delta d_2/d_2$=0.015, PSNR = 26.1 dB and its enlarged fragment

Conclusions

In the paper, we propose a new approach to phase masks optimization combining two Fresnel lenses and a cubic component. Presence in the optimized mask of pixels of two Fresnel lenses, which are calculated for two very different wavelengths, provides mostly the same defocus (blurring) for whole range of wavelength. It allows to carry out inverse imaging with more stable PSFs and to obtain images with better quality for a focus distance.

The proposed approach for MPM design provides essentially better (on 8 dB and more) PSNR of images for a focus distance than for single lens optical systems.

. It is demonstrated by numerical analysis that the proposed approach significantly increases robustness of MPMs to Gaussian additive noise introduced due to fabrication errors.

Acknowledgment

This work was supported by the Academy of Finland, project no. 287150, 2015-2019.

References

[1] Soskind, Y. G. Field Guide to diffractive optics, Bellingham: SPIE, 2011.

[2] Heide, F., Fu, Q., Peng, Y., Heidrich, W. Encoded diffractive optics for full spectrum computational imaging, Scientic Reports, 6:33543, doi:10.1038/srep33543, 2016, 10 p.

[3] Dowski, E.R., Cathey, W.T. Extended depth of field through wavefront coding, Appl. Opt., Vol. 34, No. 11, 1995, 1859-1866.

[4] Peng, Y., Fu, Q., Heide, F., Heidrich, W. The diffractive achromat full spectrum computational imaging with diffractive optics, ACM Trans. Graph., Vol. 35, No. 4, Article 31, 2016, 11 p.

[5] Katkovnik, V., Ponomarenko, M., Egiazarian, K. Lensless broadband diffractive imaging with improved depth of focus: wavefront modulation by multilevel phase masks, Journal of Modern Optics, 66 (3), 2019, pp. 335-352.

[6] Goodman, J.W. Introduction to Fourier Optics, Roberts Company Publishers, 3rd edition, 2005.

[7] Mohammad, N., Meem, M., Shen, B., Wang, P., Menon, R. Broadband imaging with one planar diffractive lens, Scientific reports, 8(1), 2799, 2018, 6 p.

[8] Dowski, E.R., Cathey, W.T. Extended depth of field through wavefront coding, Applied optics, Vol. 34, No. 11, 1995, 1859-1866.

[9] Cathey, W.T., Dowski, E.R. New paradigm for imaging systems, Applied optics, 41, 2002, 6080-6092.

[10] Katkovnik, V., Migukin, A., Astola, J. Backward discrete wave field propagation modeling as an inverse problem: toward perfect reconstruction of wave field distributions, Applied optics, vol. 48, No. 18 , pp. 3407-3423, 2009.

[11] Dabov, K., Foi, A., Katkovnik, V., Egiazarian, K. In Image restoration by sparse 3d transform-domain collaborative filtering, Proc. SPIE Electron. Imag., San Jose, CA, vol. 6812, 2008, 681-692.

JOIN US AT THE NEXT EI!

IS&T International Symposium on

Electronic Imaging

SCIENCE AND TECHNOLOGY

Imaging across applications . . . Where industry and academia meet!

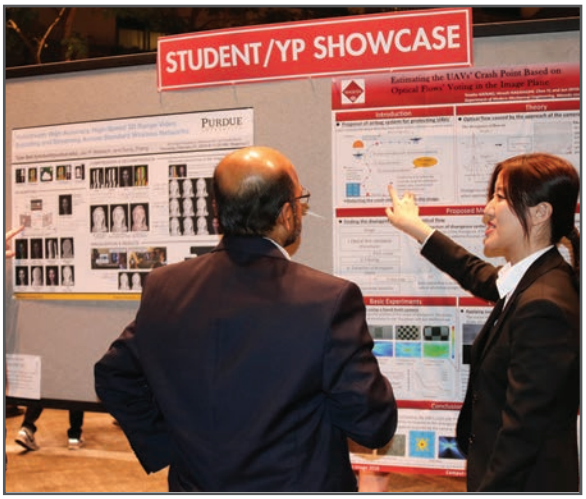

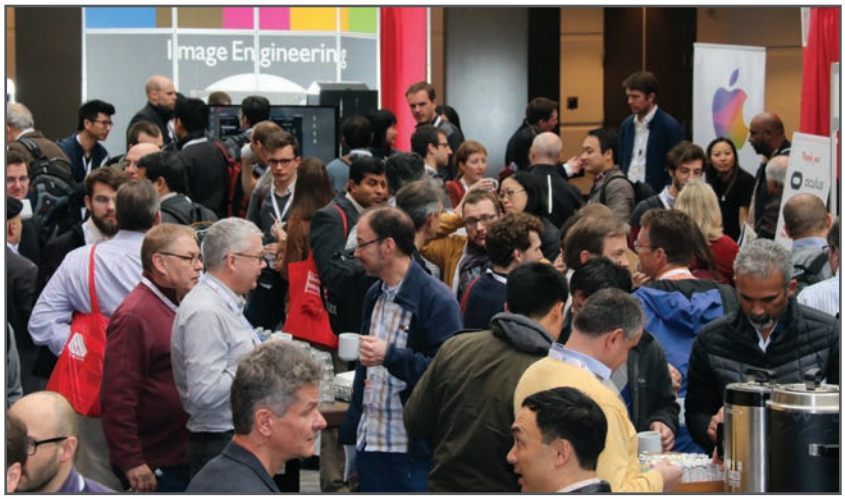

• SHORT COURSES • EXHIBITS • DEMONSTRATION SESSION • PLENARY TALKS •
• INTERACTIVE PAPER SESSION • SPECIAL EVENTS • TECHNICAL SESSIONS •

www.electronicimaging.org

IS&T
imaging.org